Investigating The Coexistence of Superconductivity and Ferromagnetism in Heterostructures

Omar Hassan
Under The Supervision of
Mr. Vladimir Zhaketov

JINR University Center
Interest Program
November 2021

Abstract

Using the experimental method of polarized neutron reflectometry through the REMUR spectrometer at the IBR-2 reactor in JINR, and combined with simulations of different nominal structures using matlab we study the correlation between experimental and theoretical data regarding certain phenomena associated with heterostructures containing superconducting and ferromagnetic layers (S-F Layers) and examine the dependency of the reflectivity of the neutron beam on different aspects of the structure.

Contents

1 Introduction

1.1 Supeconductors and Ferromagnets

Superconductivity and ferromagnetism are generally two non correlated electromagnetic phenomena, superconductivity is when at a certain critical temperature a material's electrical resistance vanishes and magnetic flux are expelled. Superconductivity is a very widely studied phenomenon in condensed matter physics both on the scale of theoretical research and industrial applications. Meanwhile, ferromagnetism is the alignment of the magnetic moments of a material's unpaired electrons producing a net magnetic moment for the material. ferromagnetism is the reason for existence of so-called permanent magnets that we see and use in everyday life as refrigerator magnet.

1.2 Interplay between the two phenomena and proximity effect

One of the first noticed apparent interplays between the two phenomena appeared in the study of change of magnetic states of layered heterostructures at different temperatures for example Pd(2 nm)/V(36.5 nm)/17[Fe(1 ML)/V(1 ML)]/10[Fe(4.7 nm)/V(4.7 nm)/MgO, where a decrease in magnetization is noticed below the critical temperature of vanadium [1]. Others structures have been investigated as V(39 nm)/20 [V(3 nm)/Fe(3 nm)] across a range of temperature where a change in magnetic states both across the plane of the structure and along its depth has been observed [2].

This change in magnetization is predominantly due to the proximity effect. As electrons in a superconductors are arranged differently than in normal metal below critical temperature through their pairing as cooper pairs and because of the non locality of the electrons and the transparency of the wave function at

the boundary between two layers of a superconductors and an ordinary metal cooper pairs can occur between electrons of the layers causing magnetization of the domain structure and demagnetization of the cluster system, with the total magnetic moment of the structure tending to zero [4]. There is also other phenomena that emerge due to this interplay in the study of phase transitions and magnetic behavior as triplet superconductivity, spontaneous vortex phase, inverse proximity effect and ferromagnetism [11].

1.3 Polarized neutron reflectometry and investigation methods

Historically, polarized neutrons were used in the study of the magnetic properties of ferromagnets by neutron depolarization method where the polarization of the transmitted neutron beam through the sample was measured. currently neutron reflectometry is used on a larger scale for different investigations as magnetic excitations in ferromagnets, structures of magnetic materials, and investigation of solid body surfaces.

Fundamentally, the theory behind neutron reflectometry is the scattering of scalar quantum particle with the potential function as the interaction potential between neutrons in the neutron beam and the materials constituting the sample.

The apparatus structure is essentially a reactor (source of neutrons), a polarizer(magnetic supermirrors, transmission through polarized gas as He, or transmission through magnetized films), a spin flipper (space varying magnetic field that is constant in time, a combination of radio frequency and constant fields), the sample, another spin flipper followed by a polarization analyzer, and finally a detector.

The detector involves two parts which are secondary radiation channels

which registers secondary radiation from the sample (charged particles, gamma quanta, and fission fragments, spin flip neutrons,and scattered neutrons by the nuclei) and we use this detection part for determination of nuclear profile for example the nuclear profile of Gd layer in Nb(15nm)/V(70nm)/Gd(3,6,12nm)/Nb(100nm)//Al2O3. The second part is the polarized neutrons which we use to study the magnetic profile of the ferromagnetic and superconducting layer.

2 Methodology

2.1 Data used and modelling

In this examination of the studied phenomenon both experimental, and theoretical data were used. Experimental data from the REMUR spectrometer at the IBR-2 reactor in JINR, and theoretical modelling was done computationally through a simulation Matlab program developed by Mr. Vladimir Zhaketov for modelling of different outputs as reflectivity, transmission, and spin asymmetry given certain input parameters as the magnetization of different layers, the thickness of each layer, interaction potential of each layer, and the magnetic field.

As it is also insightful to examine the behaviour of x-rays as compared to neutrons, and x-ray spectrometer simulator was used which included a built in database for different materials which was used to form a sample of layers/ superlattices.

2.2 Fitting of experimental data

Using data on the reflectivity of the plus and minus polarized neutrons collected by the REMUR spectrometer at two different temepratures (1.5K, 12K) for the nominal structure Al2O3 / Nb(100nm) / Gd(3nm) / V(70nm) / Nb(15nm) ,

about 700 points of data on neutrons were collected on a wavelength range between 0.5-22 angstrom corresponding to which reflectivity of the plus and minus beams were calculated (normalized by the Maxwell distribution of empty beam), then we calculated the spin asymmetry using the formula

$$SA = \frac{R_+ - R_-}{R_+ + R_-}$$

Where SA is the spin asymmetry, R_+ is the reflectivity of the plus neutrons, R_- is the reflectivity of the minus neutrons. Then we obtained the reflectivity for the neutrons using the simulation program at different parameter in attempt to obtain the best possible fit between theory and experiment. Since the critical temperature of Vanadium is 5.45K, a magnetization of 0 for the Vd layer was used, but as we predict magnetization for the part of Vanadium layer close to Gd below the critical temperature, we used a magnetization of 200 for the section of the layer close to Gd (10 nm of the 70 nm) in attempt to improve the fit, and following are the results:

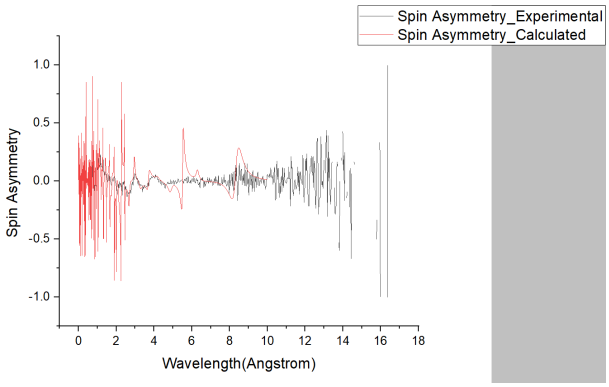

(a) $T = 12K$

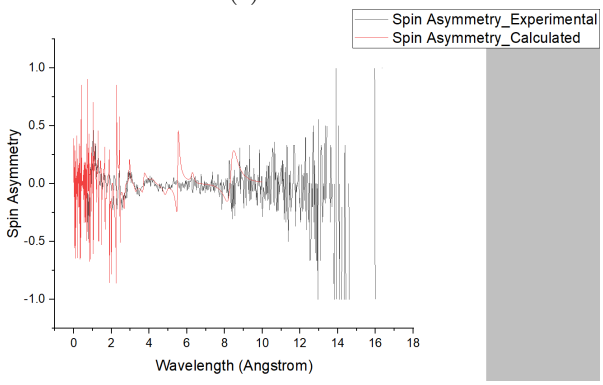

(b) $T = 1.5K$

Figure 1: Experimental and Theoretical spin asymmetry at 1.5K and 12K

As apparent, both theory and experiment tend to agree in peeks and dips throughout the plot, and we also notice large variation in the spin asymmetry at the end part of the experimental plot which is due to the small numbers of the neutrons at this range of wavelength (above 10 angstrom).

2.3 Dependence of reflectivity on grazing angle of neutron beam

In this part we examine through simulation how different grazing angles for the beam affects the reflectivity of the neutrons, for this part we use a sample of

Al2O3 / Nb(100nm) / Gd(3nm) / V(70nm) / Nb(15nm) with 0 magnetization for all layers (so we expect the graph of plus and minus neutrons to be almost identical due to the absence of magnetization), and we compare reflectivity at 3 grazing angles $\theta = 3, 6, 12$ mrad for that we following curves:

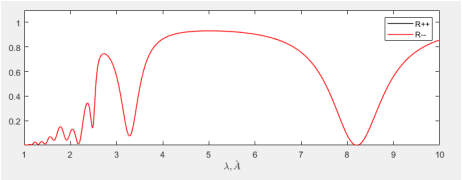

(a) $\theta = 3$ mrad

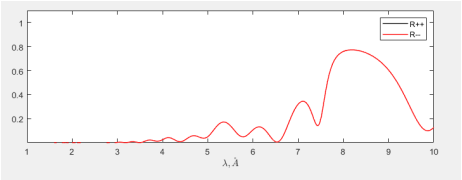

(b) $\theta = 9$ mrad

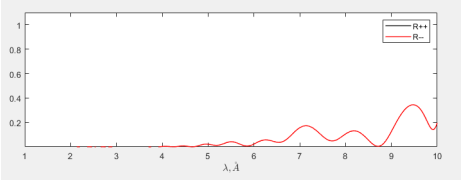

(c) $\theta = 12$ mrad

Figure 2: reflectivity at grazing angles $\theta = 3, 6, 12$ mrad

From that we observe the following within the this range of angles:

1- The peak of the graph shifts towards larger wavelength as we increase the grazing angle.

2-The amplitude of reflectivity tends to decrease as we increase the angle.

3- The red and black curves (plus and minus neutrons) are almost exactly alligned, which as we predicted is attributed to the absence of magnetization.

2.4 Dependence of reflectivity on Magnetization of ferromagnetic layer

In modelling of the magnetization of Gd (Ferromagnetic layer) there is multiple parameters that we need to consider as the collinearity of the magnetization, and its magnitude for that we examined 6 cases 3 of which we had $M_x = M_y = 0$ and $M_z = (100, 1000, 10000)$ (Collinear Magnetization) and 3 others we added a constant $M_z = 1000$, $M_y = 0$, and $M_x = (100, 500, 100)$ (Non-collinear Magnetization). In this case the magnitude of the grazing angle is fixed at $\theta = 6$ mrad for the sample Al2O3 / Nb(100nm) / Gd(3nm) / V(70nm) / Nb(15nm).

For the collinear case we got the following plots for reflectivity:

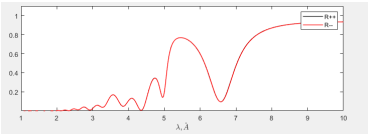

(a) $(M_x, M_y, M_z) = (0, 0, 100)$

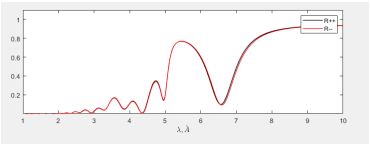

(b) $(M_x, M_y, M_z) = (0, 0, 1000)$

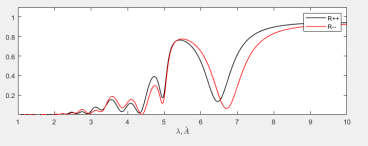

(c) $(M_x, M_y, M_z) = (0, 0, 10000)$

Figure 3: Collinear magnetization

For the non-collinear case we got the following plots for reflectivity:

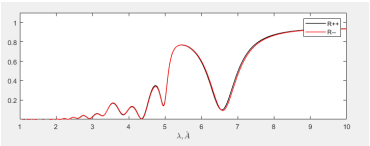

(a) $(M_x, M_y, M_z) = (100, 0, 1000)$

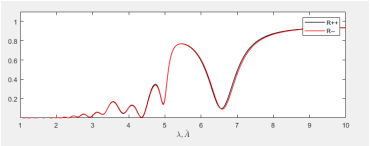

(b) $(M_x, M_y, M_z) = (500, 0, 1000)$

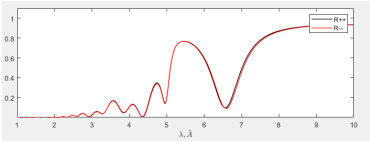

(c) $(M_x, M_y, M_z) = (1000, 0, 1000)$

Figure 4: Non-collinear magnetization

From the plots we observe the following:

1- The difference between black and red curves (plus and minus neutrons) becomes more prominent and apparent as the strength of magnetization increases, which is justifiable as the two neutron kinds differ by a magnetic property.

2- The dips and peeks in reflectivity almost coincide for different magnetization (occur at the same wavelengths), unlike the previous case for different grazing angles

3- Reflectivity tends to approach 1 for the larger wavelengths

2.5 Dependence of reflectivity on thickness of ferromagnetic layer

This analysis is rather straight forward, we vary the thickness of Gd layer in the same sample as previous section at the same grazing angle in the absence of any form of magnetization we do this for thickness 3,6, and 12 nm and observe how reflectivity is influenced. However we measure the reflectivity for both the neutrons (plus and minus) and a simulated X-ray spectrometer for the same sample.

For the neutrons we get the following plots:

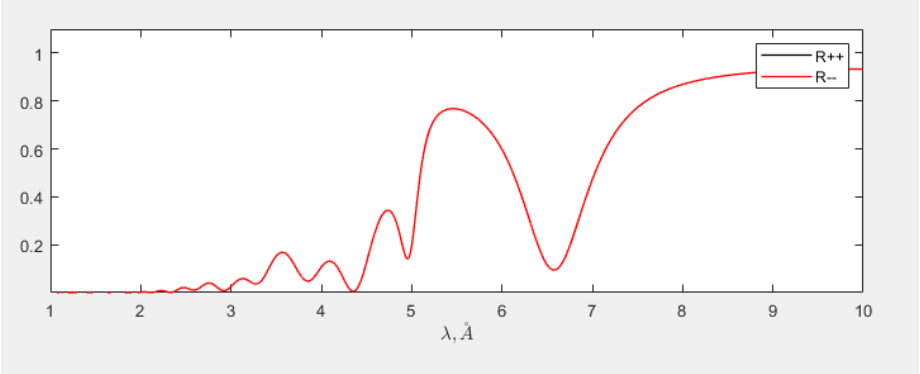

(a) $Gd = 3nm$

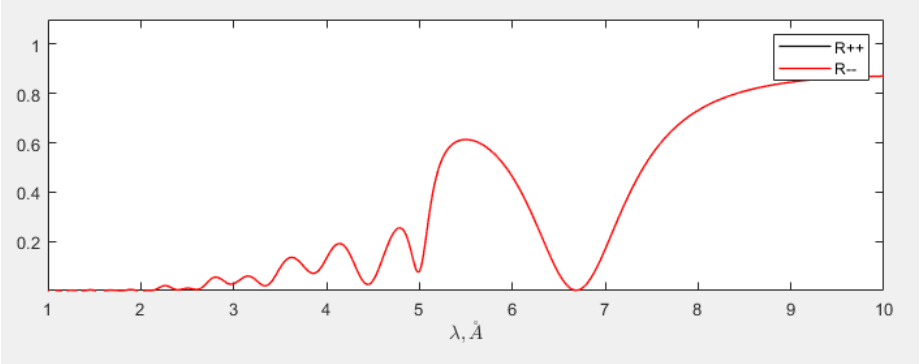

(b) $Gd = 6nm$

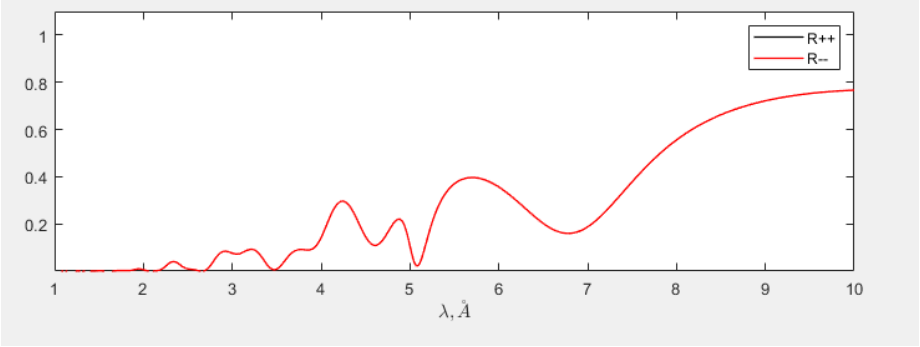

(c) $Gd = 12nm$)

Figure 5: Neutron reflectivity at different thicknesses of Gd layer

and for X-ray reflectivity we get the following plots:

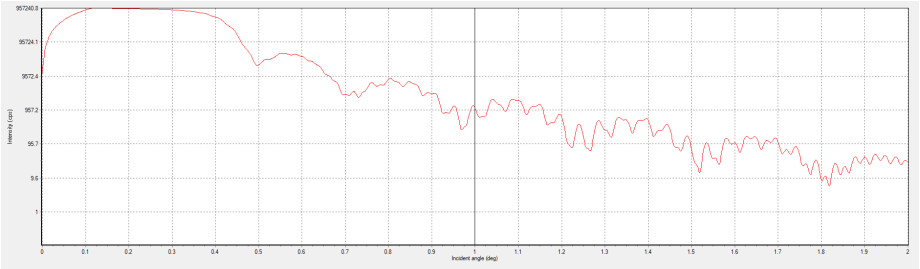

(a) $Gd = 3nm$

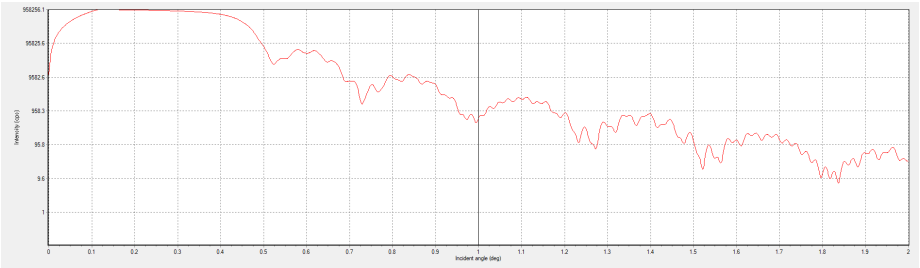

(b) $Gd = 6nm$

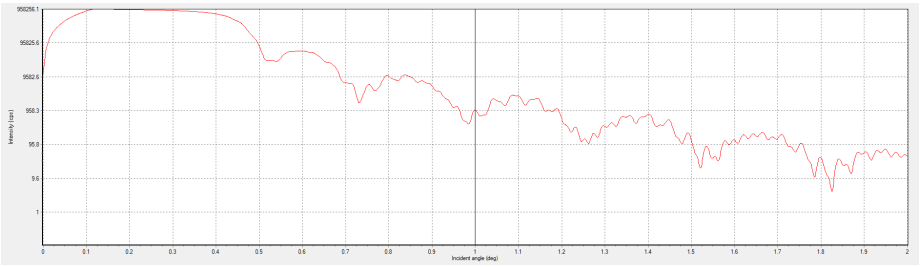

(c) $Gd = 12nm$)

Figure 6: X-ray reflectivity at different thicknesses of Gd layer

From the plots we observe:

1- For X-ray, reflictivity tends to decrease with increase of incidence angle, in agreement with the formula $Q = \frac{4\pi\theta}{\lambda}$ for small θ where reflectivity is proportional to $\frac{1}{Q^4}$

2-For neutrons, increasing thickness tends to lower the peaks of the reflectivity (amplitude of the peak between 5-6 angstroms decreases as thickness increase)

2.6 Reflectivity at different ferromagnets

In this section we investigate how the interaction potential between neutrons/X-rays and ferromagnetic layer affects the reflectivity by changing the the ferromagnet Gd,Fe,Co,Ni,Dy each of which has different scattering length density (resembles the interaction potential) all of which were in the sample Al2O3 / Nb(100nm) / X(3nm) / V(70nm) / Nb(15nm), where X is the ferromagnet, the grazing angle is fixed at 6 mrad and no magnetization.

The following are the reflectivity plots for neutrons:

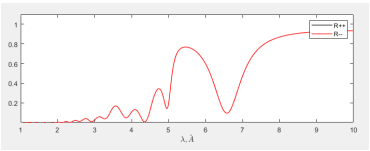

(a) Gd

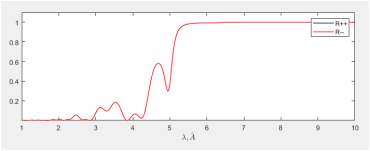

(b) Fe

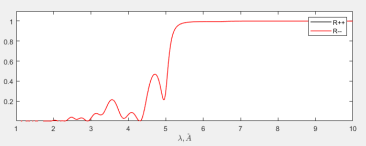

(c) Co

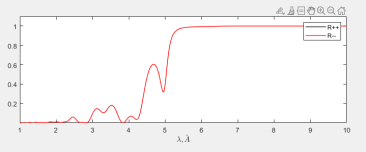

(d) Ni

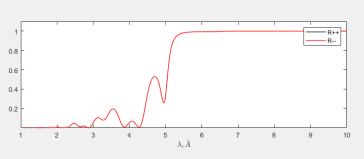

(e) Dy

Figure 7: Neutron reflectivity at different ferromagnetic layers

For X-ray we obtained the following plots:

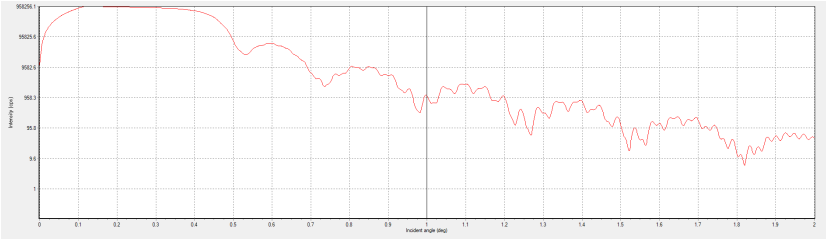

(a) Gd

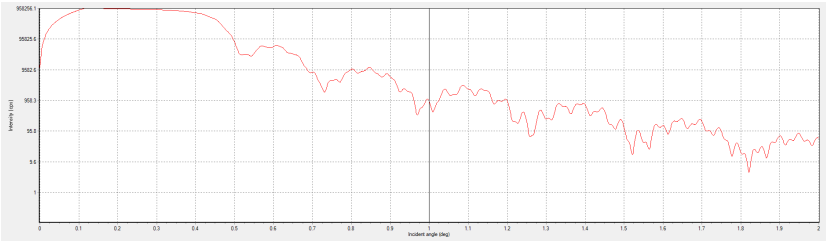

(b) Fe

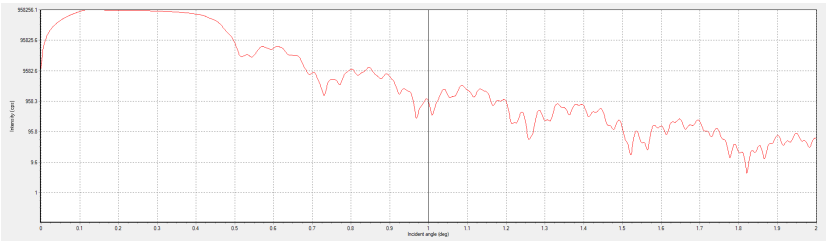

(c) Co

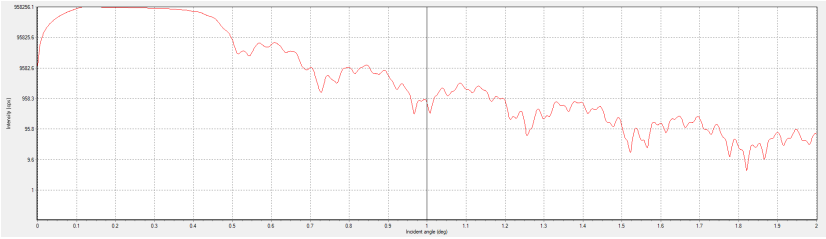

(d) Ni

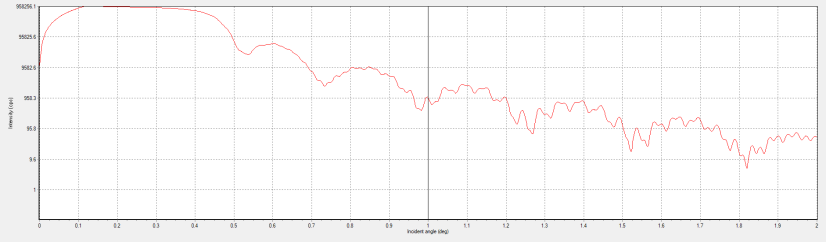

(e) Dy

Figure 8: X-ray reflectivity at different ferromagnetic layers

We notice the similarity between (Fe-Ni-Co) in both reflictivities as they are neighbors in the periodic table, We also notice how reflectivity approaches 1 for wavelengths > 5 angstrom except for Gd which could be attributed to a characteristic of Gd as a certain absorption energy.

2.7 Reflectivity of superlattices

Superlattices are formed by repeating of the S-F layer (superconductor-ferromagnet) multiple times for example Al2O3 / [Nb(25nm) / Gd(3nm)] x10 / Nb(15nm) where effects in superlattices tend to be more prominent compared to normal lattices so its insightful to examine the reflectivities for the case of super lattices. We used the superlattice Al2O3 / [Nb(25nm) / Gd(3nm)] / Nb(15nm) where [Nb(25nm) / Gd(3nm)] is repeated 10,20,30 times. Following are plots for neutron reflictivities:

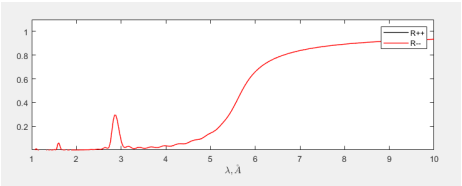

(a) Nb-Gd=10x

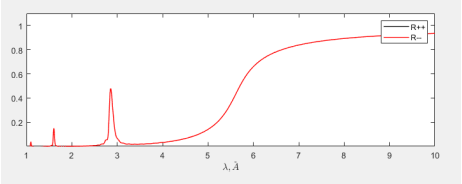

(b) Nb-Gd=20x

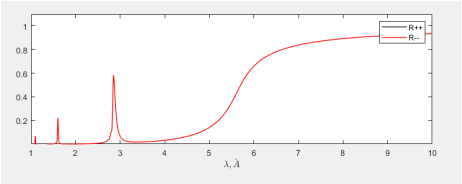

(c) Nb-Gd=30x

Figure 9: Neutron reflectivity at 10x,20x,30x supperlattice

Notice how the spikes (peaks) near wavelengths 1.1, 1.5, 2.9 angstrom are increased in the neutron reflectivity plots as we gradually increase the repetition of Nb-Gd layer from 10x to 20x to 30x, this is an example of how superlattices show effects and anomalies better. For the case of X-ray we get the following plots:

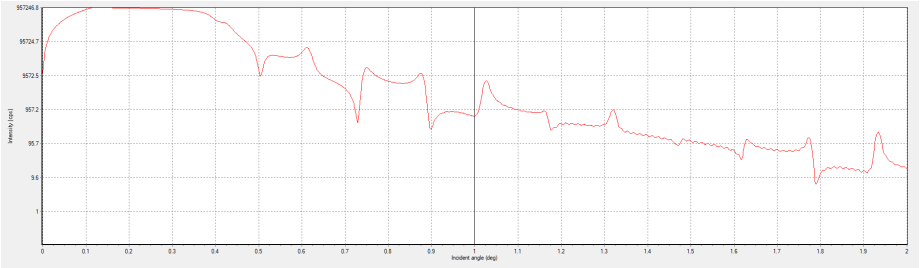

(a) Nb-Gd=10x

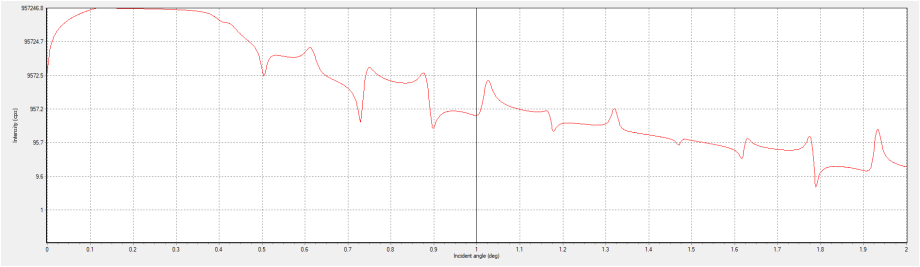

(b) Nb-Gd=20x

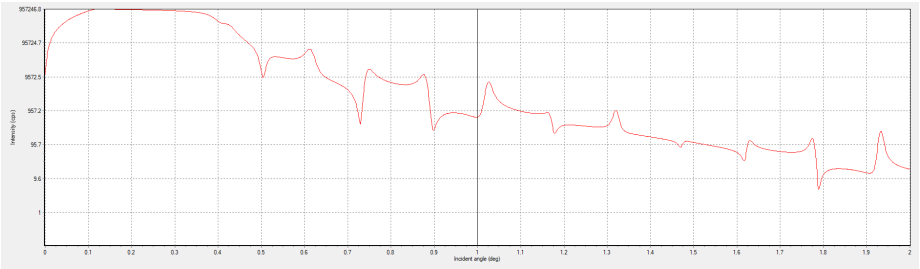

(c) Nb-Gd=30x

Figure 10: X-ray reflectivity at 10x,20x,30x supperlattice

Notice how the graph in the case of X-ray becomes more refined and smooth as we increase repetition of Nb-Gd layer, we clearly observe that the curve at 10x is much more "granular" and patchy as compared to the 30x graph.

Also to make effects more apparent we plot the reflectivity of x-ray, and plot as linearized graph.

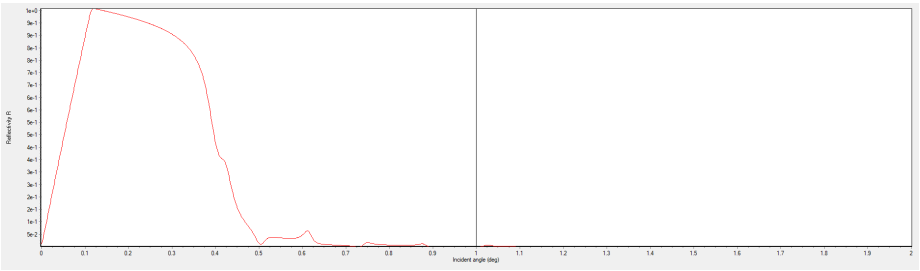

(a) Nb-Gd=10x

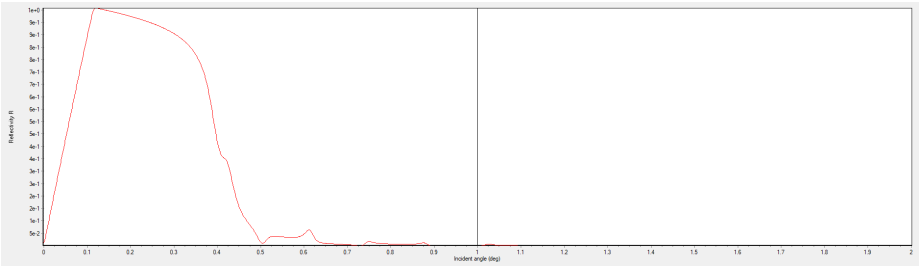

(b) Nb-Gd=20x

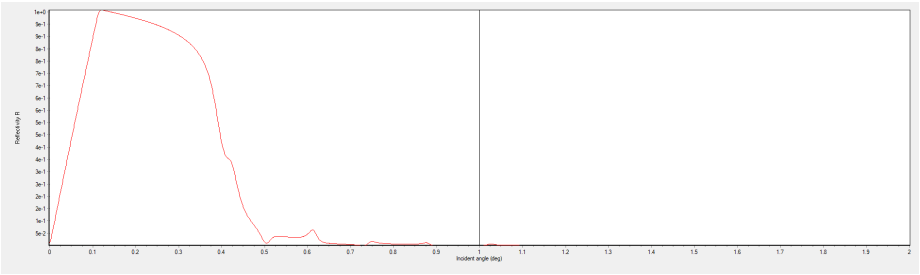

(c) Nb-Gd=30x

Figure 11: X-ray reflectivity (as Y-axis,linear) at 10x,20x,30x supperlattice

Notice how the bragg peaks become more apparent in this plot, and as we increase the number of repitition of Nb-Gd layer.

2.8 Effect of roughness of ferromagnetic layer on reflectivity

In this section we only use X-ray simulation, and we investigate how changing the roughness of Gd layer between 0,1,2,3 nm in the sample Al2O3 / [Nb(25nm) / Gd(3nm)] x20 / Nb(15nm) affects the reflectivity curve. Following are plots of the X-ray reflectivities at different roughness:

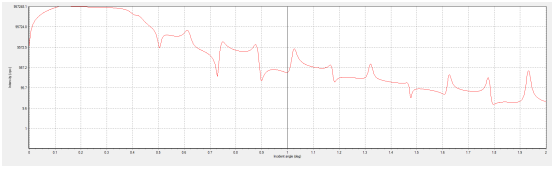

(a) roughness=0

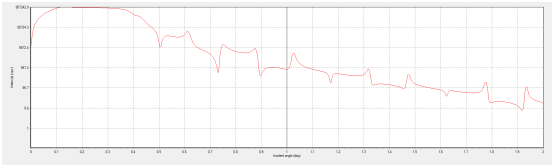

(b) roughness=1

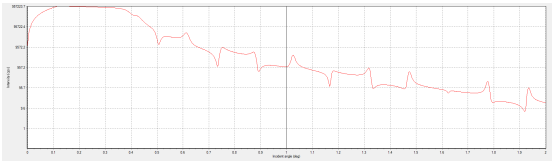

(c) roughness=2

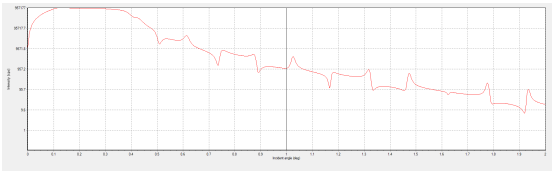

(d) roughness=3

Figure 12: X-ray reflectivity at different roughness of Gd layer

2.9 Ferromagnetic layers of helicoidal magnetization

For the last simulation we used the matlab program simulating the neutron reflectivity to examine the super lattice of the nominal structure Al2O3 / Nb(100nm) / Dy(3nm) / V(70nm) / Nb(15nm) setting the values of the magnetization Dy layer to form a helicoid. This was done by splitting the 3nm layer into 20 0.15nm sublayers whose z and x components of magnetization form a helical structure of for constant magnitude M where each layer i had M_x and M_z given by $M_x(i) = MCos(\theta(i))$, $M_z(i) = MSin(\theta(i))$ where $\theta(i)$ is the angle the magnetization vector M(i) of the ith layer makes with the x- axis. We did this for two magnitudes of M (100,100000) and the results were as follows:

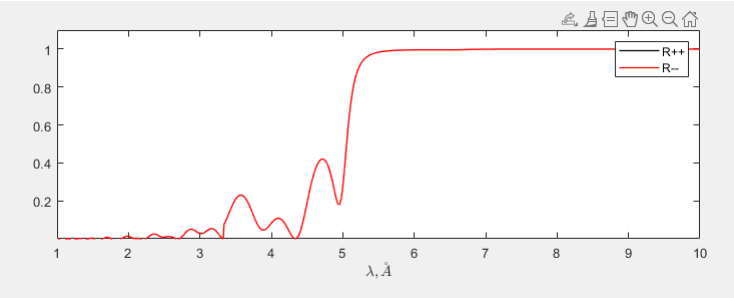

(a) M=100

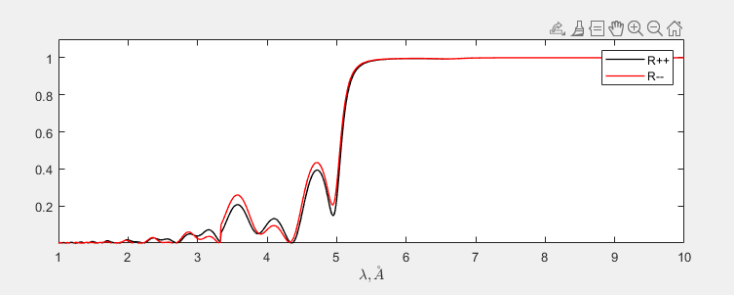

(b) M=100000

Figure 13: Helicoidal magnetization of magnitude M of Gd layer

We notice how the separation between plus and minus beams become more apparent for the larger magnetization magnitude.

3 Conclusion

In summary, neutron reflectometry is a powerful method to study multiple aspects of the behavior of superconductors and ferromagnets in a given nominal structure where measuring reflectivity throughout different parameters as temperature, layers' thickness, grazing angle of the neutrons, interaction potential, magnetization, superlattices, and roughness gave us insight as to how these parameters affect the reflection of the polarized neutrons where several effects as the change in magnetization below critical temperature of the super conductor is observed by fitting of experimental and theoretical data in agreement with the proximity effect, how superlattices make effects more prominent, the behaviour of different ferromagnets in the sample , etc.

4 References

[1]Aksenov, V. L., Jernenkov, K. N., Khaidukov, Y. N., Nikitenko, Y. V., Petrenko, A. V., Proglyado, V. V., ... & Wäppling, R. (2005). Interplay between superconductivity and ferromagnetism in Fe/V multilayered structure studied by polarized neutron reflectometry. Physica B: Condensed Matter, 356(1-4), 9-13. [2]Aksenov, V. L., Nikitenko, Y. V., Petrenko, A. V., Uzdin, V. M., Khaidukov, Y. N., & Zabel, H. (2007). Features of the magnetic state of the layered Fe-V nanostructure of the superconductor-ferromagnet type. Crystallography Reports, 52(3), 381-386.

[3]Aksenov, V. L., Nikitenko, Y. V., Khaidukov, Y. N., Vdovichev, S. N., Borisov, M. M., Morkovin, A. N., & Mukhamedzhanov, E. K. (2009). Coexistence of superconductivity and ferromagnetism in the Nb (500 Å)/Fe (39 Å)/[Si (34 Å)/Mo (34 Å)] 40/Si nanostructure. Journal of Surface Investigation. X-ray, Synchrotron and Neutron Techniques, 3(4), 495-499.

[4]Aksenov, V. L., Khaidukov, Y. N., & Nikitenko, Y. V. (2010, February). Peculiarities of magnetic states in ferromagnet/superconductor heterostructures due to the proximity effects. In Journal of Physics: Conference Series (Vol. 211, No. 1, p. 012022). IOP Publishing.

[5]Salikhov, R. I., Garif'Yanov, N. N., Garifullin, I. A., Tagirov, L. R., Westerholt, K., & Zabel, H. (2009). Spin screening effect in superconductor/ferromagnet thin film heterostructures studied using nuclear magnetic resonance. Physical Review B, 80(21), 214523.

[6]Khaydukov, Y. N., Perov, N. S., Borisov, M. M., Mukhamedzhanov, E. K., Csik, A., Zhernenkov, K. N., ... & Aksenov, V. L. (2012). Structural and magnetic properties of the periodic [Fe (5nm)/V (5nm)] 10 and [Fe (3nm)/V (3nm)] 20 systems. In Solid State Phenomena (Vol. 190, pp. 396-400). Trans Tech Publications Ltd.

[7]Khaydukov, Y. N., Nagy, B., Kim, J. H., Keller, T., Rühm, A., Nikitenko, Y. V., ... & Aksenov, V. L. (2013). On the feasibility to study inverse proximity effect in a single S/F bilayer by polarized neutron reflectometry. JETP letters, 98(2), 107-110.

[8]Zhaketov, V. D., Nikitenko, Y. V., Radu, F., Petrenko, A. V., Csik, A., Borisov, M. M., ... & Aksenov, V. L. (2017). Magnetism in structures with ferromagnetic and superconducting layers. Journal of Experimental and Theoretical Physics, 124(1), 114-130.

[9]Zhaketov, V. D., Nikitenko, Y. V., Petrenko, A. V., Csik, A., Aksenov, V. L., & Radu, F. (2017). Relaxation of the magnetic state of a ferromagnetic–superconducting layered structure. Journal of Experimental and Theoretical Physics, 125(3), 480-494.

[10]Zhaketov, V. D., Nikitenko, Y. V., Petrenko, A. V., Vdovichev, S. N., Churakov, A. V., & Csik, A. (2018). Reflexivity and Correlation of Magnetic

States of Nanostructures in the Nb (70 nm)/Ni 0.65 Cu 0.35 (6.5 nm)/Si Ferromagnet–Superconductor Heterostructure. Journal of Experimental and Theoretical Physics, 127(3), 508-515.

[11]Zhaketov, V. D., Nikitenko, Y. V., Khaidukov, Y. N., Skryabina, O. V., Csik, A., Borisov, M. M., ... & Churakov, A. V. (2019). Magnetic and Superconducting Properties of the Heterogeneous Layered Structures V/Fe sub 0.7 V sub 0.3/V/Fe sub 0.7 V sub 0.3/Nb and Nb/Ni sub 0.65 (0.81) Cu sub 0.35 (0.19). Journal of Experimental and Theoretical Physics, 129(2).

[12]Khaydukov, Y. N., Vasenko, A. S., Kravtsov, E. A., Progliado, V. V., Zhaketov, V. D., Csik, A., ... & Keimer, B. (2018). Magnetic and superconducting phase diagram of Nb/Gd/Nb trilayers. Physical Review B, 97(14), 144511.

[13]Khaydukov, Y. N., Kravtsov, E. A., Zhaketov, V. D., Progliado, V. V., Kim, G., Nikitenko, Y. V., ... & Keimer, B. (2019). Magnetic proximity effect in Nb/Gd superlattices seen by neutron reflectometry. Physical Review B, 99(14), 140503.

[14]Khaydukov, Y., Kravtsov, E., Morari, R., Lenk, D., Mustafa, L., Kim, G., ... & Keimer, B. (2019, November). Neutron reflectometry studies of Gd/Nb and Cu30Ni70/Nb superlattices. In Journal of Physics: Conference Series (Vol. 1389, No. 1, p. 012060). IOP Publishing.

[15]Mironov, S., Mel'nikov, A. S., & Buzdin, A. (2018). Electromagnetic proximity effect in planar superconductor-ferromagnet structures. Applied Physics Letters, 113(2), 022601.

[16]Logoboy, N. A., & Sonin, E. B. (2009). Superconductivity without diamagnetism in systems with broken time-reversal symmetry. Physical Review B, 79(2), 020502.

[17]Anderson, P. W. (1962). Theory of flux creep in hard superconductors. Physical Review Letters, 9(7), 309.

[18]Bergeret, F. S., Efetov, K. B., & Larkin, A. I. (2000). Nonhomogeneous magnetic order in superconductor-ferromagnet multilayers. Physical Review B, 62(17), 11872.

[19]Gu, Y., Halász, G. B., Robinson, J. W. A., & Blamire, M. G. (2015). Large superconducting spin valve effect and ultrasmall exchange splitting in epitaxial rare-earth-niobium trilayers. Physical review letters, 115(6), 067201.